Meteoritics 28, 538–551 (1993)

Trace elements in mineral separates of the Peña Blanca Spring aubrite: Implications for the evolution of the aubrite parent body

K. LODDERS[1], H. PALME AND F. WLOTZKA

Max-Planck-Institut für Chemie, Abt. Kosmochemie, Saarstraße 23, D-6500 Mainz, Germany
[1]Present address: Dept. of Earth and Planetary Sciences, Washington University, St. Louis, Missouri 63130, USA

(Received 1993 January 15; accepted in revised form 1993 June 3)

Abstract–The origin of the aubrite parent body (APB) and its relation to the enstatite chondrites is still unclear. Therefore we began a detailed chemical study of the aubrite Peña Blanca Spring. Bulk samples and mineral separates (oldhamite, troilite, alabandite, pyroxene) of Peña Blanca Spring were analyzed for major and trace elements by instrumental neutron activation analysis (INAA). In addition, a leaching experiment was performed on a powdered bulk sample to study the distribution of trace elements in aubrite minerals.

The elemental abundances in Peña Blanca Spring are compared to abundances in EH-chondrites and EL-chondrites in an attempt to distinguish volatility related fractionations (evaporation, condensation) from planetary differentiation (melting and core formation). Low abundances of siderophile (*e.g.*, Ir) and chalcophile (*e.g.*, V) elements in bulk samples indicate that 25% (by mass) metal and about 6% (by mass) sulfide separated from an enstatite chondrite like-parent body to form a core and a residual mantle with aubrite composition. We argue that the high observed rare earth element (REE) abundances in oldhamite (>100 x EH-chondrite normalized) reflect REE incorporation into oldhamite during nebular condensation. Thus, oldhamite in aubrites is, at least in part, a relict phase as originally proposed by Lodders and Palme (1990). Some re-equilibration of CaS with silicates has, however, occurred, leading to partial redistribution of REE, as exemplified by the uptake of Eu by plagioclase.

The distribution of the REE among aubritic minerals cannot be the result of fractional crystallization, which would occur if high degrees of partial melting took place on the APB. Instead, the REE distributions indicate incomplete equilibrium of oldhamite and other phases. Therefore, a short non-equlibrium melting episode led to segregation of metal and sulfides.

INTRODUCTION

A total of 14 enstatite achondrites (aubrites) is known. The Peña Blanca Spring aubrite is one of nine observed falls. This highly reduced meteorite fell on 1946 August 2 with a "violent splash" into a swimming pool at the Gap ranch in Brewster County, Texas, and pieces with a total mass of about 70 kg were collected (Lonsdale, 1947).

Aubrites contain a suite of exotic sulfur-bearing minerals, such as oldhamite (CaS), that are sensitive to decomposition by water. However, the rapid removal of the meteorite from the swimming pool and the fact that the meteorite did not break up into small pieces minimized the damage to this brecciated rock. Nevertheless, oxidation of iron bearing sulfides occurred rapidly and led to small brownish spots of iron-oxide around the remaining iron sulfides in the white and gray enstatite host material.

Peña Blanca Spring, like other aubrites, consists predominantly of Fe-free pyroxene (>90 vol%, see Table 1), with gray colored enstatite being more abundant than white appearing enstatite. Peña Blanca Spring contains the largest enstatite crystals (10 x 7.5 x 6 cm) ever described in an aubrite (Lonsdale, 1947). Other silicates, such as diopside, forsterite, and plagioclase are minor constituents and are randomly dispersed in the enstatite groundmass (Lonsdale, 1947; Watters and Prinz, 1979). Silica-rich "albitic" glass inclusions in orthopyroxene were also reported (Fuchs, 1974).

Kamacite (Fe,Ni), troilite (FeS), and ferroan-alabandite ((Mn,Fe)S) are present as small grains in the enstatite matrix at an abundance level below 1 vol%. Oxidation products from mm-sized grains of these phases are responsible for the orange-brown colored areas. Other sulfides such as djerfisherite ($K_3(Cu,Na)(Fe,Ni)_{12}(S,Cl)_{14}$), daubreelite ($FeCr_2S_4$), and caswellsilverite ($NaCrS_2$) are intergrown with troilite and/or alabandite. Also present in small amounts is oldhamite which occurs in sulfide associations or as single grains in the matrix.

TABLE 1. Modal abundances (vol.-%) and plagioclase composition of Peña Blanca Spring.

	(1)	(2)
enstatite	93	95.4
plagioclase	0.5	2.1
diopside	5	2.7
forsterite	0.5	0.3
kamacite	0.5	tr
troilite	1.25	tr
oldhamite	-	tr
other	0.25	
sum	101	100.5
An (mole-%)	12	3.06
Ab (mole-%)	88	94.5

(1) Lonsdale (1947). (2) Watters and Prinz (1979).

Most researchers agree that aubrites formed by igneous processes on a parent body rather than by condensation from a reduced solar gas. For example, Watters and Prinz (1979) suggest that aubrites formed through fractional crystallization on an EL-chondrite-like parent body. Based on extensive mineralogical studies of the Norton County aubrite, Okada *et al.* (1988) also concluded that aubrites formed by fractional crystallization. However, the observed bulk REE patterns, which are either displaying negative, positive, or no Eu anomalies (*e.g.*, Wolf *et al.*, 1983) are inconsistent with fractional crystallization. The production of the "classical aubritic negative Eu anomaly" cannot be explained by fractional crystallization as the low concentrations of Ca and Al in E-chondrites would not allow crystallization and subsequent removal of plagioclase from an enstatite chondritic melt. In general, modeling of aubrite petrogenesis is complicated because of the highly reduced

nature of these rocks and the unusual chemistry of their mineral phases with elements such as Ca, Ti, Na, K, and the REE partially present as sulfides.

In this paper we report analytical data for major and trace elements in various phases of Peña Blanca Spring. We then discuss the implications of the trace element abundances for the formation conditions of a metal-sulfide core and for the evolution of the aubrite parent body in general.

EXPERIMENTAL

Samples

A 5 x 1.5 x 1-cm chunk of the Peña Blanca Spring aubrite (from the MPI meteorite collection in Mainz) was carefully cut without using water. About 7.7 g were powdered in an agate mill and an aliquot of 240 mg was used for instrumental neutron activation analysis (INAA). About 200 mg were used for a leaching experiment. Another piece (11.4 g) was gently crushed and troilite, ferroan-alabandite, oldhamite, and white and gray pyroxene fractions were separated by handpicking under a binocular microscope.

Two oldhamite grains, identified by a greenish coating, were collected: a larger grain weighing 4.11 mg and about 1.5 mm in diameter, and a smaller grain weighing 0.097 mg and about 0.3 mm in diameter.

Two samples of troilite, which occurs as golden brownish 50–500 μm sized grains were prepared (2.08 mg and 4.06 mg). Alabandite fractions (1.29 mg and 2.85 mg) were separated by handpicking the black-bluish appearing sulfides, which are generally smaller than troilite grains and are weakly magnetic.

Instrumental Neutron Activation Analysis (INAA)

All samples were analyzed by INAA using the standard method of the Mainz Cosmochemistry Group (*e.g.*, Wänke *et al.*, 1977). The samples were irradiated in polyethylene capsules for 6 h at a thermal neutron flux of 7 x 10^{11} n s^{-1} cm^{-2} in the carousel of the TRIGA Mark II reactor at the Johannes-Gutenberg Universität Mainz. After irradiation samples were counted several times in different geometries on large Ge(Li) detectors. The gamma-spectra obtained were evaluated using the peak-fitting routine of Kruse (1979). Concentrations were calculated by irradiating and counting appropriate standards under identical conditions.

For leaching, the activated powdered sample was treated stepwise with 20 ml each of water, 5% aqueous NH_4Cl, and 1N HCl for 60 min at 80 °C. The solutions obtained were counted on Ge(Li) detectors to determine the fractions of elements dissolved.

SEM Studies

After irradiation and INAA, polished sections were prepared (without using water) from the separated oldhamites, troilite fractions, white pyroxene, from additional gray pyroxene and from a larger chunk of whole rock. These sections were studied first with an optical microscope and then with a scanning electron microscope (SEM Hitachi 450) equipped for energy dispersive X-ray analysis (EDS). Quantitative analyses of minerals were performed using analyzed mineral standards (Jarosewich *et al.*, 1980) and stoichiometric, meteoritic FeS. The results were corrected using standard ZAF correction methods (Quant-X program by KEVEX).

RESULTS AND DISCUSSION

Results of the INAA and SEM-EDS studies, together with literature data, are given in Tables 2-4, additional data from SEM-EDS analyses are shown in Table 5.

Bulk Composition of Peña Blanca Spring

Bulk analyses from this study and literature data are summarized in Table 2. In general, the abundances are within

TABLE 2. Bulk elemental abundances in Peña Blanca Spring.*

Reference - sample #	Mg	Al	Si	Ca	Ti	Na	S	K	Sc	V	Cr	Mn	Fe	Co	Ni	Cu	Zn	As	Se	Sb	Cs	Ir	Au
	wt.-%	wt.-%	wt.-%	wt.-%	wt.-%	ppm	wt.-%	ppm	ppm	ppm	ppm	ppm	wt.-%	ppm	ppm	ppm	ppm	ppb	ppm	ppb	ppb	ppb	ppb
This work, 240 mg[1,2]	21.07	0.77		0.68[a]	<0.03	4990	0.49	245[a]	6	6.6[b]	530	1170	0.53	2.2	40[b]	<30	<20	1200[b]	2.2[a]	<10	580	0.9[c]	1.5[b]
Biswas et al. 1980														0.6		8.74	2.54	153	1.23		353		
Easton 1985	22.5	0.37	27.13	0.93	0.09	2400	0.2	320			620	1620	0.31	2	50								
Gibson et al. 1985							0.25																
Schmitt et al. 1972		0.23				1360			5.2		370	1180	<0.7	4		9							
Spettel, 210 mg[3]	23.84	0.29	26.75	0.86	0.04	3160	0.26	240	9	6.4	620	1940	0.96	9.8	146				2.37		530	4.6	7
Strait 1983 - I						1280			5.4		140		0.21	1.31							170		
Strait 1983 - II						2000			6.1		320		0.55	1.72	39						240		0.7
Strait 1983 - III						1960			36.5		80		0.28	1.5							390		
Strait 1983 - IV						410			4.9		190		0.2	0.7	22						160		1.2
Watters & Prinz 1979	23.2	0.24	27.7	0.59	0.006	1780	0	80				460	0.05	0	0								
Wolf et al. 1983 - I									6.2		386		0.6	1.41	22				1.53	4.9	220	0.31	3.4
Wolf et al. 1983 - II									6.2		386		0.6	1.41	22		1.64		0.18	2.17	159	0.0207	3.84

*see Table 4 for REE analyses. [1] 1σ- error for INAA: no indices: < 6%, a: 6-10%, b: 10-20%, c: 20-30%. [2]Sulfur data by G. Dreibus (pers. comm.). [3]Analysis by B. Spettel, MPI Mainz.

the ranges of reported literature values. However, our sample has higher abundances of Al, Na, Fe, and S than found in most other analyses. These differences will be discussed in the sections below.

Elemental abundances in Peña Blanca Spring and the average abundances in EL-chondrites are plotted in Fig. 1, normalized to Al and to EH-chondrites. Normalization to Al is preferred because of the Si/Mg fractionation in enstatite chondrites (*e.g.*, Larimer and Wasson, 1988) and because Si is partly sited in the metal phase (*e.g.*, Keil, 1968; Watters and Prinz, 1979).

Abundances are normalized to EH-chondrites because the aubrite precursor material probably had greater affinity to the highly reduced enstatite chondrites than to the more oxidized carbonaceous chondrites. The abundance pattern of moderately volatile elements in EH-chondrites shows characteristic differences from the abundance pattern in carbonaceous chondrites (*e.g.*, Palme *et al.*, 1988). Abundances of Au, P, and Ga in EH-chondrites are higher than in CI-chondrites (when normalized to Si) by as much as a factor of 1.4 in the case of Au. Thus enstatite chondrites are fractionated relative to solar (CI) abundances. These differences cannot be easily understood and may depend on fractionations under extremely reducing conditions. Because aubrites probably formed by differentiation of an enstatite chondrite-like parent body it is more appropriate to normalize to EH-chondrites than to CI-chondrites.

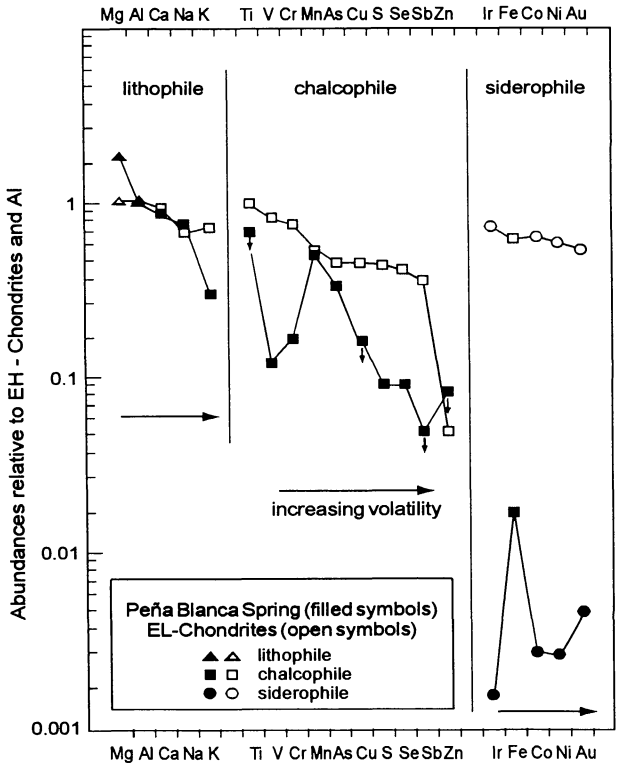

FIG. 1. Bulk composition of Peña Blanca Spring (INAA) and average composition of EL-chondrites normalized to EH-chondrites and Al. Elements are listed in order of increasing volatility within the groups of lithophile, chalcophile, and siderophile elements. In the group of lithophile elements, Ca, Na, and K are plotted with the symbol for chalcophile elements to indicate their partial occurrence in sulfides. The S-data for Peña Blanca Spring are from G. Dreibus (1991; pers. comm.), data for EH- and EL-chondrites from Wasson and Kallemeyn (1988).

By normalizing to EH-chondrites we obtain a measure of volatility related elemental fractionations under extremely reducing conditions. The primitive EH-chondrites have higher contents of volatile and moderately volatile elements than the EL-chondrites. It is very likely that this difference reflects nebular condensation processes in a highly reduced gas where the enstatite meteorites formed. Differences in the abundances of moderately volatile and volatile elements between EH- and EL-chondrites then provide a measure of the type and extent of depletion either by volatilization or incomplete condensation under highly reducing conditions. In Fig. 1, elemental abundances are plotted in the order of decreasing EL/EH-chondritic ratios within the groups of lithophile, chalcophile, and siderophile elements. Elements which are depleted below the level of Fe, Co, and Ni in EL-chondrites may be assumed to be volatile under reducing conditions. The arrangement in Fig. 1 will be helpful for distinguishing between volatility related processes and metal-sulfide segregation in explaining the observed elemental abundances in aubrites.

It is important to keep in mind that relative to each other, refractory elements such as Al, Ca, Sc, and the REE have the same abundances in CI-chondrites or EH-chondrites. However, refractory element abundances normalized to Si are lower by a factor of 2 in enstatite chondrites when compared to CI-chondrites. For the sake of consistency, all abundance data in this paper are given relative to EH-chondrites.

Refractory elements—In Fig. 1 and 2, the abundances of Sc, Al, Ca, Ti, V, and some REE are shown relative to EH-chondrites. Abundance patterns for refractory elements are similar whether normalized to EH- or CI-chondrites. The chondritic Yb/Lu ratio excludes high temperature volatility related effects, because under reducing conditions Yb is much more volatile than Lu (Lodders and Fegley, 1993). The only refractory element depleted in Peña Blanca Spring is V. As will be discussed later, the large V depletion of a factor of ten most likely indicates sulfide separation on the APB. Only upper limits were obtained for Ti, another potential indicator of sulfide separation.

In our bulk sample the Al (and also Na) abundance is higher than previous reported values (Table 2). In aubrites, albite is the main host for Al and Na ($Ab_{>90}$, Watters and Prinz, 1979).

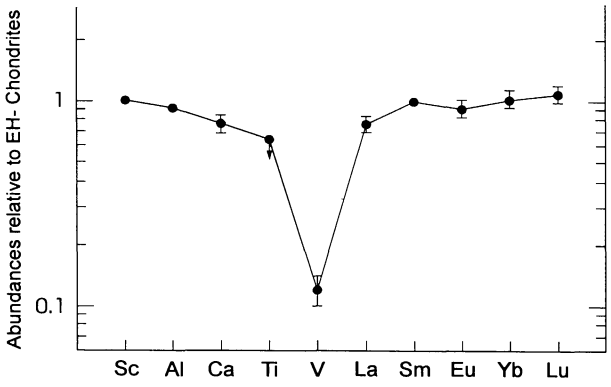

FIG. 2. Refractory elements in Peña Blanca Spring relative to EH-chondrites. The depletion of V is remarkable and must be ascribed to sulfide separation on the APB.

TABLE 3. Elemental abundances in mineral separates of Peña Blanca Spring.*

Phase	Reference	Mg	Al	Si	Ca	Ti	Na	S	Cl	K	Sc	V	Cr	Mn	Fe	Co	Ni	Cu	Zn	Se	Sb	Ir	Au
		wt.-%	wt.-%	wt.-%	wt.-%	wt.-%	ppm	wt.-%	wt.-%	ppm	ppm	ppm	ppm	ppm	wt.-%	ppm	ppm	ppm	ppm	ppm	ppb	ppb	ppb
enstatite (wh)	INAA 17.62 mg[1]	21.08	0.31		4.09	0.052[b]	1780			80[b]	18.9	<1.4	32	130	0.023[b]	<0.3							
enstatite (gr)	INAA 30.52 mg[1]				<0.4	<0.07	1100			90[a]	4.5		268	510	0.41	3	100[a]		12[b]			3[b]	4[a]
enstatite	Lonsdale 1947	24	0.14	27.69	0	0								0	0.45								
enstatite	Reid & Cohen 1967	24.25	0.06	27.53	0.31	0							70	720	0.04		30						
enstatite	Watters & Prinz 1979	24	0.04	27.95	0.41	<0.01	150						205	465	0.05								
diopside	Watters & Prinz 1979	12.1	0.29	26.55	15.73	0.11	2000						140	390	0.05								
forsterite	Lonsdale 1947	29.36	0.12	23.76	0.03	0.05									0.27								
forsterite	Watters & Prinz 1979	34.38	0	19.8	0.07									155	<0.02		<160						
albite	Watters & Prinz 1979	0.01	10.8	31.41	0.39	0.01	86800			4730					<0.02								
silicates	Easton 1985	23.13	0.38	29.95	0.5	0	2220			290			634	152	0.01								
alabandite	INAA 1.29 mg[1]					1.2[a]	740			1290[a]	41.9		10000	167000	38.8	406	1460[a]	590[a]	183[a]	115	<1.2	20	<3
alabandite	INAA 2.85 mg[1]					0.53[b]	1570			730	33.1		57530	248200	21.6	14.4	430[b]	350[a]	806	120	<0.02	20	31
djerfisherite	SEM-EDS[1]							35.48	1.24	86700			<1300	<600	52.84		6400[c]	9600[b]					
djerfisherite	SEM-EDS[1]							34.7	12.1[a]	84000			1130[b]	<4700	52.11		16000	8500[b]					
djerfisherite	El Goresy et al. 1974						0	32.6	18	106000					51.9		14000	13000	tr				
djerfisherite	El Goresy et al. 1974						3000	32.7	15	109000					50.4		7000	14000	tr				
oldhamite[2]	INAA 0.097 mg[1]	<1.9	0.5		39.74	<0.3	1180			<190	84.5	100[b]	1080[a]	16300	1.72[c]	190		<50	<160	130[b]			
oldhamite	EDS (0.097 mg grain)[1]	0.58[b]			53.86	0		44.57						11100[a]	0.16[b]								
oldhamite[2]	INAA 4.11 mg[1]	<1.8	<0.1		45.34	<0.44	920			<150	28.5	<24	1640	22800	1.6	30		<100	100[b]	200			
oldhamite	EDS (4.11 mg grain)[1]				54.11	0		44.47						12400	.13-.25								
oldhamite	Watters & Prinz 1979	0.89		<0.02	54.3	0.12		44.5					<200	<200	<0.02				<200				
troilite	INAA 2.08 mg[1]					1.3[b]	320			620[a]	0.9[a]		9490	4140	56	5.7	480[b]	460	65[b]	130	0.3[b]	35[c]	81
troilite	INAA 4.06 mg[1]	<0.3	0.014[b]		0.09[b]	1.2	70			390	0.4[b]	795	8330	1200	55.64	1.1	275[c]	370	27[b]	140	<0.4	<26	
troilite	SEM					0.9-1.7		37.94					3000[c]	0-0.05	60.44								
troilite	Watters & Prinz 1979	0.05		0.03	0.11	3.15		36.9					9000	1200	59.2								
metal	Easton 1985														96.6	1400	35500						
metal	Easton 1986														96.34	1400	35200						
metal	Lonsdale 1947													1700	95.74	3900	42200	0					
metal	Wasson & Wai 1970			<0.007													61000						
metal	Watters & Prinz 1979[3]			0.12											95.4	2500	37000						

*see Table 4 for REE analyses. [1]1σ- error for INAA and SEM-EDS analysis: no indices: < 6%, a: 6-10%, b: 10-20%, c: 20-30%. [2]Oldhamite grains contain troilite and alabandite, see Table 5 and text.
[3]Watters and Prinz (1979) list the identical analysis for the Cumberland Falls aubrite.

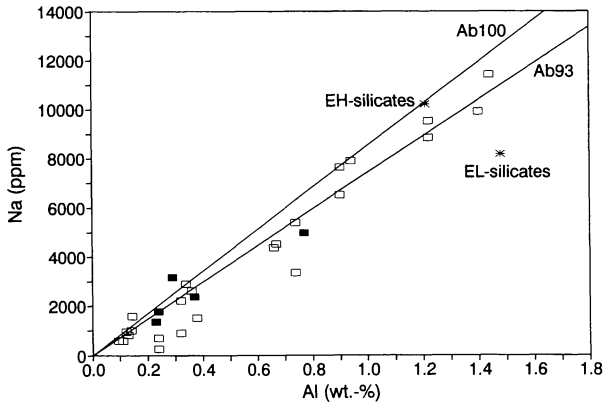

FIG. 3. Whole rock Na and Al abundances in Peña Blanca Spring (filled symbols, data see Table 2) and other aubrites (data mainly from Easton 1985; Schmitt *et al.*, 1972; Strait, 1983; Watters and Prinz, 1979). Aubrites show a wide range of Na and Al abundances and the good Na *vs.* Al correlation indicates that albitic plagioclase is the main host for Na and Al. The lines correspond to pure albite and the average plagioclase composition in aubrites (Watters and Prinz, 1979). For comparison, data for Na and Al abundances in the silicate portions of EH- and EL-chondrites calculated from data by Wasson and Kallemeyn (1988) and Keil (1968) are also plotted.

A survey of aubrite literature analyses reveals that Na and Al abundances in aubrites range from 590 to 11,400 ppm Na and 0.095 to 1.44 wt% Al and that Na and Al correlate well. This correlation is shown in Fig. 3. All data follow the correlation and therefore the higher Al and Na abundances in our sample must be explained by higher albite contents. The good correlation of Na with Al in bulk samples and the Na/Al ratio found in individual plagioclase indicates that Na is more or less quantitatively contained in plagioclase, and the fraction of Na in sulfide must be very small. Because aubrites likely formed from enstatite-chondrites as parent material, the Na and Al abundances in the silicate portions of EH- and EL-chondrites are also shown in Fig. 3 for comparison. Most of the aubrite samples are depleted in Al (relative to chondrites), and it is therefore commonly stated that plagioclase removal occurred on the APB (*e.g.*, Wilson and Keil, 1991). However, this statement needs to be reconsidered because several aubrites (*e.g.*, Bishopville, Bustee, Khor Temiki, Mayo Belwa) show Al (and Na) abundances similar to those in silicate portions of enstatite chondrites (Strait, 1983; Easton, 1985; Watters and Prinz, 1979).

Lithophile elements—As illustrated in Fig. 1, some of the lithophile elements (Ca, Na, K, Si) show chalcophile or siderophile tendencies but their major fraction is located in silicates. The abundances of Na and K in EL-chondrites are at about the same level as Fe, Co, and Ni suggesting that both Na and K are only slightly volatile under highly reducing conditions. The depletion of K relative to Na in the bulk aubrite sample is probably not a result of volatility related processes because the volatility of K is not very different from Na and processes affecting K should also reduce the Na content. Instead, the depletion of K may be due to removal of djerfisherite, a sulfide that contains up to 10% K, but only about 0.3% Na (Table 3). If we assume an EH-chondritic K abundance for the entire aubrite parent body, the observed Na/K fractionation could be achieved by removal of about 0.5 wt% of djerfisherite into the core, while the Na abundance in the silicate remains almost unchanged.

EH-chondrite normalized REE abundances of bulk Peña Blanca Spring show a flat pattern. However, as shown in Fig. 4 and Table 4, different REE patterns were also reported. The occurrence of different REE patterns reflects heterogeneous sampling. The REE are concentrated in the minor phases oldhamite and plagioclase (see below), so that bulk REE patterns mainly depend on the amount of oldhamite and/or plagioclase in the sample and the REE abundance level in the host phases. The apparently random amounts of plagioclase and oldhamite in bulk Peña Blanca Spring samples may not be surprising, considering the brecciated nature of this meteorite. Mass balance calculations for REE will be discussed below.

Siderophile elements—Elements such as Co, Ni, Ir, and Au are depleted by more than a factor of 100 relative to Al normalized EH-chondrite abundances (Fig. 1), indicating almost complete metal removal from the bulk sample. Their low abundances in bulk samples and the good elemental correlations among them suggest they are entirely sited in the metal phase (Table 2). Indeed, no metal particles could be separated for INAA. In the polished sections only one small metal fragment with a few percent Ni was found, but it was too small for a precise Ni analysis by EDS.

We grouped Fe, which occurs as metal and sulfide in aubrites, as a siderophile element because in E-chondrites the major fraction of Fe is present as metal. The varying Fe (and S) abundances (Table 2) must be due to varying amounts of metal and troilite enclosed in bulk samples. Our sample contained mm-sized inclusions of troilite while metal could not be detected. The low Ni abundance also indicates that no significant metal was included. Therefore, the relatively high Fe abundance (Fig. 1) must be ascribed to troilite. In contrast, the sample analyzed by B. Spettel (Table 2) contained more metal and less sulfide as indicated by the higher Fe and Ni but smaller S content.

Chalcophile elements—Elements with chalcophile character, such as Ti, V, Cr, Mn, As, Cu, S, Se, Sb, and Zn are depleted by factors between 0.5–0.05x Al normalized EH-chondrites

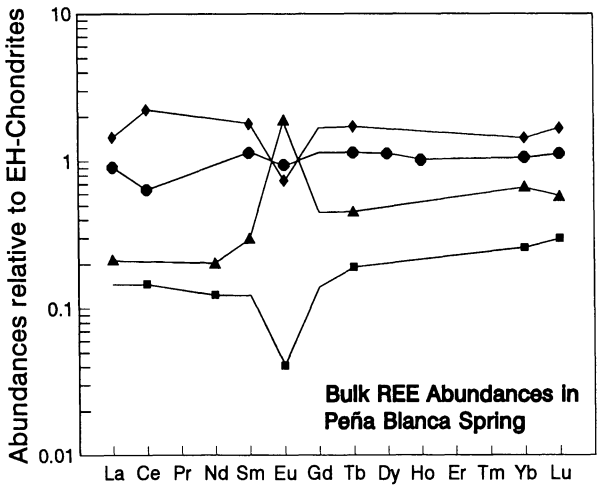

FIG. 4. REE in whole rock samples of Peña Blanca Spring relative to EH-chondrites. Normalization to CI-chondrites results in the same patterns. Different bulk REE patterns indicate sampling problems to obtain a representative bulk analysis in aubrites. Source of data (see also Table 4): Circles: this work; diamonds: unpublished data MPI für Chemie, Mainz (B. Spettel); triangles: Strait (1983); squares: Wolf *et al.* (1983).

TABLE 4. REE in whole rock samples and mineral phases of Peña Blanca Spring (all data in ppm).

Phase	Reference - sample #	La	Ce	Nd	Sm	Eu	Tb	Dy	Ho	Yb	Lu
bulk	This work, 240 mg[1]	0.19[a]	0.42[b]		0.16	0.051[b]	0.04[b]	0.27[b]	0.051[a]	0.17[a]	0.027[a]
bulk	Spettel, 210 mg[2]	0.34	1.47		0.25	0.04	0.06			0.23	0.04
bulk	Srait 1983 - I	0.051	0.38	0.094	0.042	0.103	0.016			0.108	0.014
bulk	Srait 1983 - II	0.154			0.077	0.044	0.134				0.024
bulk	Strait 1983 - III	0.827	3.75		2.08	0.092	0.622			1.83	0.269
bulk	Strait 1983 - IV	0.061			0.023	0.035	0.033			0.079	0.019
bulk	Wolf et al. 1983 (I+II)		0.097	0.057		0.0022	0.0067			0.041	0.0072
enstatite (white)	INAA, 17.62 mg[1]	0.15[c]			0.13	0.02[c]		<0.07	0.05[b]	0.2[b]	0.04[c]
enstatite (gray)	INAA, 30.53 mg[1]	0.37[a]			0.11	0.04[a]		0.09[c]	0.03[b]	0.11[b]	0.02[b]
oldhamite	INAA, 4.11 mg[1]	83.8	294[a]	203	73.5	5.4	18[b]	108[b]	22[b]	61.7	9.1
oldhamite	INAA, 0.097 mg[1]	21.3[a]	85[b]	53[c]	24.3	5.8	7.1[b]	37.5[a]	8	21.6[a]	3.1[a]
oldhamite	Benjamin et al. 1984		30	20							
troilite	INAA, 2.08 mg[1]	3.44[a]			0.086[b]	0.083[b]					
troilite	INAA, 4.06 mg[1]	0.13[b]			0.12	0.018[a]		0.16[b]	0.03[c]	0.14[c]	0.04[c]
alabandite	INAA, 1.29 mg[1]	1.26[a]			0.69	<0.07			0.2[b]	0.88[a]	0.15[c]
alabandite	INAA, 2.85 mg[1]	0.56[b]			0.24[a]	0.13[c]				0.6[b]	0.1[b]

[1]1σ- error for INAA: no indices: <6%, a: 6-10%, b: 10-20%, c: 20-30%. [2]Analysis by B. Spettel, MPI Mainz.

Fig. 1). In ordinary and carbonaceous chondrites, which formed under less reducing conditions, some of these elements are lithophile (*e.g.*, Ti, V, Cr, Mn, Zn).

The abundance level of As and Sb are clearly above the abundance level of siderophile elements such as Fe, Co, and Ni, indicating that As and Sb seem to be more chalcophile than siderophile. Metal/silicate partition coefficients for As and Sb are about 5−10x higher than that for Co (Lodders and Palme, 1991). If As and Sb were primarily siderophile, metal segregation would have depleted As and Sb below the Co abundance level. However, the observed abundances of As and Sb are higher and fall within the range of other chalcophile elements, implying that both elements are contained in sulfides together with other chalcophile elements such as V, Cr, Mn, and Cu.

In comparing the trace element abundance pattern of bulk Peña Blanca Spring with the volatility sequence defined by the EH- to EL-chondritic ratios we note large deviations of V, Cr, and perhaps Ti. The abundance sequence of V, Cr, and Mn is opposite to the expected volatility depletion sequence and therefore most likely reflects sulfide separation.

The abundance pattern for more volatile elements (As-Zn) in Peña Blanca Spring follows the volatility trend predicted by the EL/EH-chondritic ratios. For these elements volatility related processes and, in addition, sulfide fractionation should be considered.

The most obvious deviation from volatility-produced depletions in less reduced systems is the large depletion of Zn in EL-chondrites, where Zn is 10x lower in abundance than S and Se. By contrast, in carbonaceous chondrites CI-normalized Zn abundances are similar to S and Se (Palme *et al.*, 1988). The low Zn abundance in both EL-chondrites and aubrites may indicate that Zn becomes highly volatile under extremely reducing conditions. In Peña Blanca Spring only an upper limit of about 20 ppm could be obtained for Zn. Biswas *et al.* (1980) report 2.5 ppm Zn implying that Zn is depleted by a factor of ten relative to S and Se, just as in EL-chondrites.

Leaching Experiment

The results of stepwise leaching procedures of a powdered bulk sample are presented in Fig. 5. The fractions of elements dissolved in water, aqueous NH_4Cl, and HCl relative to the bulk sample are plotted. For example, all soluble Ca (about 20% of total Ca) is dissolved in water, while Cr only dissolves in HCl and does not appear in any appreciable amounts in the earlier water and NH_4Cl fractions. Most of the REE are not soluble in water but dissolve in NH_4Cl and HCl. This is surprising because the major fraction of the REE is concentrated in oldhamite which is known to be water soluble. The different solubility behavior of Ca and the REE is probably due to the different pH-dependent solubility products of Ca and REE compounds. Adding water to the sample dissolves oldhamite while the REE sulfides are probably converted to hydroxy-oxides which are not soluble in

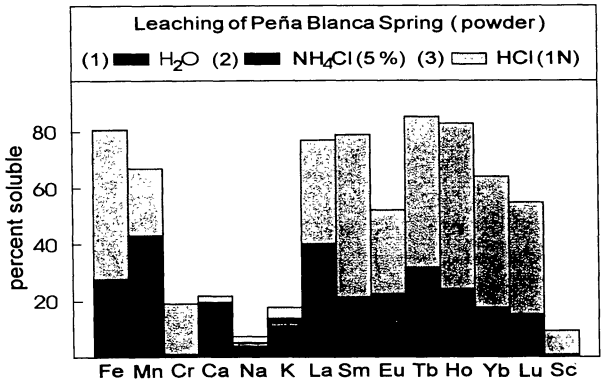

FIG. 5. Results of stepwise leaching of Peña Blanca Spring powder with water, 5% NH_4Cl, and 1 N HCl. Water is capable of removing some Na, K, Ca, and Eu, while leaching of other REE requires more acidic solutions. Note that about half of Eu and the HREE remain in the residue. This indicates that the silicate residue contains most likely plagioclase and diopside, which are potential Eu and HREE host phases, respectively.

water, but require more acidic solvents for dissolution. The same solubility behavior for Ca and the REE was found by Shima and Honda (1967) in a leaching experiment on the Abee enstatite chondrite. Based on Shima and Honda's experiments, Sears *et al.* (1983) suggested REE-precipitation during the aqueous CaS dissolution step as an explanation of why the REE and Ca are not leachable together.

Europium behaves somewhat differently than the other REE, as it partly dissolves in water together with Ca, Na, and K. These elements should therefore be most sensitive to meteorite weathering on the Earth. Kallemeyn and Wasson (1986) found that within a given enstatite chondrite group, these elements generally have lower abundances in Antarctic finds than in non-Antarctic falls. They attributed these depletions to terrestrial weathering. Because Peña Blanca Spring had already taken a "bath" on its fall, mobilization of Ca, Na, K and some of the REE certainly cannot be excluded. On the other hand, leaching was applied to powdered samples in hot solvents which favor rapid dissolution.

The fraction of REE in insoluble silicates was estimated from the leaching experiment by assuming that sulfides dissolve completely upon leaching. The EH-normalized REE pattern in the remaining silicate fraction is enriched in the HREE relative to the LREE and shows an Eu excess, indicating that the silicate contains plagioclase and diopside, which are major Eu and HREE carriers. The amount of trace sulfide phases was calculated assuming that all of the dissolved Ca, Fe, Mn, and Cr were initially present as sulfides. Mass-balance results in abundances of about 0.27 wt% CaS, 0.67 wt% FeS, 0.12 wt% MnS and 0.015 wt% Cr_2S_3 for bulk Peña Blanca Spring.

Composition of Separated Phases

Oldhamite—Results of analyses (INAA) of two oldhamite grains are given in Tables 3 and 4. The relatively high contents of Mn and Fe suggest that troilite and ferroan-alabandite are present in the separated oldhamite grains because lower Mn and Fe abundances were reported for pure aubritic oldhamite (Watters and Prinz, 1979; Wheelock, 1990). EDS-SEM analysis confirmed the presence of troilite and alabandite as rounded blebs enclosed in the oldhamite grains. In addition, caswellsilverite, either included in or associated with alabandite was identified in the larger oldhamite grain. The composition of these phases together with analyses of the pure CaS are given in Table 5. These sulfide inclusions have also been reported by Wheelock (1990) for oldhamite in Norton County, but these inclusions were not mentioned by Floss (1991) who studied oldhamites from several other aubrites. The totals for INAA data are lower than expected for stoichiometric CaS, MnS, and FeS. Other authors also had difficulties obtaining totals of 100% for oldhamite (Keil, 1968; Larimer and Ganapathy, 1987; Wheelock, 1990). This probably indicates that weathering decomposed some CaS. Weathering products form a greenish layer around the oldhamite grains whereas fresh oldhamite samples appear light-pink colored.

The REE abundances in the larger grain (4.11 mg) are about 450x EH-chondrites and in the smaller grain (0.097 mg) about 150x EH-chondrites (Table 4, Fig. 6). Both grains show a negative Eu-anomaly, with Eu abundances about 100x EH-chondritic. From the leaching experiments we estimated a bulk modal CaS abundance of about 0.3 wt%. If the REE were exclusively and homogeneously contained in oldhamite, the expected REE abundances are about 370x EH-chondritic. This is less than the level of 450x EH-chondritic in the larger CaS grain but is more than double the REE abundances in the smaller grain. Because oldhamite is randomly dispersed in the meteorite, problems are expected in obtaining a representative bulk REE analysis, especially for small bulk samples.

Both CaS grains are enriched in Sc, but the 5–15x EH-chondritic abundances are much lower than those of the REE. No data on Sc abundances in oldhamite from other aubrites are available for further comparison, but our data are similar to the Sc abundance of 8–17x EH-chondrites in oldhamite of EH-chondrites (Chen *et al.*, 1989).

Troilite—Data for major and trace elements in the two Ti-bearing troilite fractions are given in Tables 3 and 4. Both troilite fractions analyzed by INAA show variable amounts of Na, K, Cr and Mn, suggesting that other sulfide phases such as caswellsilverite, daubreelite, or alabandite are associated. SEM-EDS analyses of troilite and some of these associated phases are given in Table 5. The variable Mn and Cr abundances in troilite suggest incomplete exsolution of Cr- and Mn-sulfides from FeS. In larger troilite grains, Cr-rich lamellae are observed. The small lamellae are generally too thin to allow reasonable quantitative analysis, but they have clearly variable Cr/Fe-ratios suggesting that Cr-rich phases are due to exsolution. The associated Mn- and Cr-sulfides may be products of low temperature immiscibility from troilite so that analysis of bulk sulfide

TABLE 5. SEM-EDS analysis of sulfide phases in oldhamite grains and individual alabandite and troilite matrix grains of Peña Blanca Spring (data in wt.-%).

	Oldhamite grain (4.11 mg)				Oldhamite grain (0.097 mg)			Grains in enstatite matrix	
	CaS	(Mn,Fe)S	FeS	$NaCrS_2$	CaS	(Mn,Fe)S	FeS	FeS	(Mn,Fe)S
# analysis	8	7	3	2	6	1	2	10	2
Fe	0.16±0.02	15.84±0.7	61.16±1.1	0.06	0.13 - 0.25	13.9	61	60.44±0.4	9.1
Mn	1.11±0.07	45.41±0.9	0.12 - 0.35	0.21	1.24±0.02	47.2	0.14	0 - 0.05	52.4
Ca	53.86±0.3	0.16 - 0.41	-	0.13	54.11±0.9	1.9	-	-	-
Mg	0.58±0.07	1.47±0.6	-	-	< det. limit	0.18	-	-	0.99
Cr	-	0.13±0.02	0.18 - 0.35	27.86	-	-	0.37	0.3±0.1	0.4
Na	-	-	-	33.75	-	-	-	-	-
Ti	0	-	0.52 - 1.5	-	0	-	0.97 - 1.5	0.9 - 1.7	-
S	44.57±0.2	37.10±0.3	37.5±0.8	38	44.47±0.9	36.73	37.07	37.94±2	37.09

fractions might reflect the sulfide composition during high temperature differentiation on the APB.

A remarkable enrichment of about 15 x EH-chondritic for V was found in troilite. The high V content in troilite and the low V in bulk Peña Blanca Spring (Fig. 1) supports our conclusion that the V depletion in the bulk sample was caused by sulfide removal. Therefore, the V abundance in troilite is used below to estimate the amount of sulfide removal on the APB. Troilite is also enriched in Ti which abundance ranges from about 20 to 40x EH-chondritic. One troilite fraction shows higher amounts of Ni, Ir, and Au, suggesting that some metal is associated with the troilite grains.

One troilite fraction has REE abundances of about 0.5x EH-chondrites with a small negative Eu-anomaly and HREE enrichment (Table 4). This REE pattern is not characteristic of troilite but must be ascribed to oldhamite contamination. The amount of Ca in this troilite fraction is sufficient to explain the high REE abundances by contamination of oldhamite, considering the high REE abundance levels in the oldhamite separates (150–450x EH-chondrites). SEM analysis of the troilite grains showed the presence of a rounded, strongly weathered oldhamite grain in one of the troilite grains of this separate. The texture of this weathered area resembles that shown in Fig. 2 of Okada *et al.* (1981).

The other troilite fraction was very small, and INAA was only sensitive for determining La, Sm, and Eu. The La abundance was found to be surprisingly high (14x EH-chondrites). Because this troilite fraction also contains considerable amounts of Na and Cr, La might be sited in caswellsilverite, as suggested for E-chondrites by Kallemeyn and Wasson (1986). The relatively high amount of Na could suggest that some plagioclase is present. However, in that case Eu abundances should be much higher than that of La, which is not observed.

The smaller Sm abundance of 0.6x EH-chondrites *vs.* an 1.4 EH-chondritic Eu abundance implies a REE pattern in troilite with a positive Eu-anomaly, as predicted for FeS by experimental REE iron sulfide/silicate partition coefficients (Lodders and Palme, 1990). However, additional data on the REE abundances of pure troilite are necessary to confirm the relative Eu enrichment in troilite.

Ferroan-alabandite–Both fractions analyzed by INAA contain high but variable Mn and Fe contents (Table 3). The Mn data are lower while Fe data are higher than values reported by Watters and Prinz (1979) for aubritic alabandite (34–43%, 15–24% respectively). This suggests that the INAA separates contain associated troilite. Because alabandite also contains Mg, which was not determined by INAA, totals in both fractions (assuming stoichiometric sulfides) are only about 80–90%. In addition, SEM studies show that weathering attacks alabandite stronger than troilite (Fig. 7). Layered weathering reaction rims are found around the alabandite while the neighboring troilite is essentially unattacked.

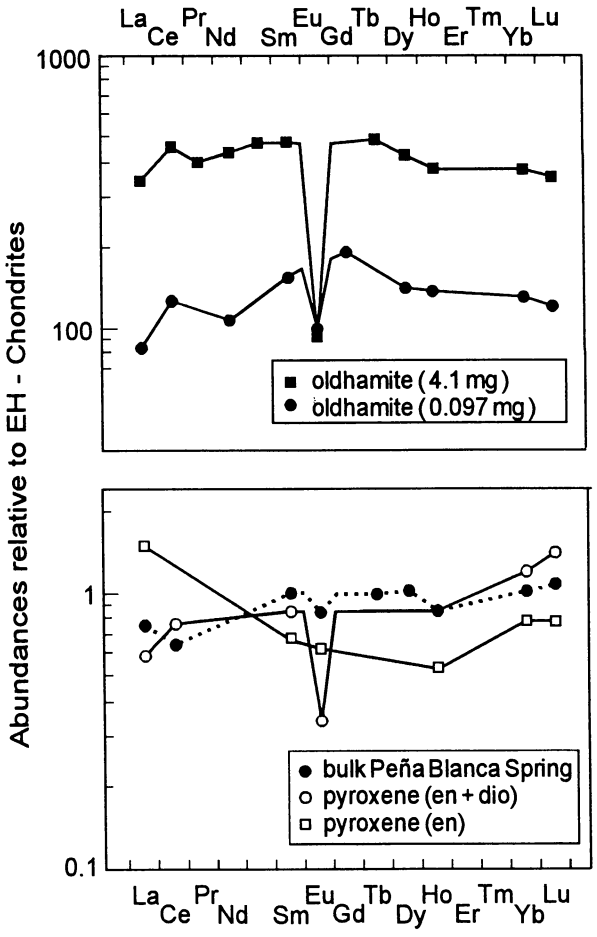

FIG. 6. REE abundances (relative to EH-chondrites) in separated phases of Peña Blanca Spring. Oldhamite is highly enriched in the REE. The REE pattern of pyroxene fractions are not typical for pyroxene and may reflect minor inclusions of other REE bearing phases. The pyroxene data therefore represent upper limits for REE only.

FIG. 7. SEM-photograph of a troilite-alabandite assemblage in Peña Blanca Spring. The alabandite (left) shows strongly weathered rims while the neighboring troilite (right) is mainly unattacked.

We also analyzed the alabandite found in polished matrix sections by SEM-EDS (Table 5). The Mn content of these samples is much higher than previously reported values and is higher than found for alabandite exsolved from oldhamite. Higher Mn contents in alabandite of pyroxenitic clasts (about 40%) than in alabandite from a sulfide (CaS) dominated clast (Mn about 28%) are also reported by Wheelock (1990).

The INAA of the REE was complicated by high background counting statistics of Mn. However, both fractions are REE enriched about 1–5x EH-chondritic. One fraction shows a relatively flat pattern about 5x EH-chondritic with a small negative Eu anomaly. The other fraction shows a more or less flat pattern at about 2–4x EH-chondrites. Patterns with LREE to HREE enrichment (0.1 to 10x chondritic) and a negative Eu-anomaly are found for Norton County alabandite by Wheelock (1990).

Pyroxenes—The major mass of Peña Blanca Spring consists of grayish appearing enstatite. The most apparent differences between the gray and the less abundant white pyroxene are the higher Fe and the lower Ca, Sc, and REE abundances in the former one (Tables 3, 4). However, the data for the gray pyroxene cannot be representative for pure enstatite because the abundances of Fe, Ni, Ir, and Zn are likely due to minute inclusions of sulfides and metal. Okada *et al.* (1988) also describe these two populations of enstatite for the Norton County aubrite and note the presence of sub-micron sized metal and sulfide inclusions.

The REE from the pyroxene fractions are within EH-chondritic abundance levels (Fig. 6). The less abundant white pyroxene is probably a mixture of enstatite and diopside, because it contains 4% Ca. It shows a flat REE pattern with a clear Eu depletion. The gray pyroxene is enriched in the LREE. This is not a typical REE-pattern for pyroxene and indicates that minor REE carrying phases, such as sulfides, are present in the sample analyzed. Therefore, the REE abundances represent only upper limits for pyroxene. In addition, the leaching experiment showed that about 20% of the total Sm is left in the residue, which consists mainly of pyroxene. This implies an upper limit of about 30 ppb of Sm for pyroxene; however, the separated fractions carry about 110–130 ppb Sm. Obviously, other REE host phases, such as trace amounts of oldhamite must be present. Only 0.1–0.3% of oldhamite inclusions with Sm abundances characteristic of the oldhamite grains analyzed here are needed to account for the excess Sm. The presence of trace CaS (0.1–0.3%) in the pyroxene fraction corresponds to only 0.05–0.16% Ca, significantly less than the observed Ca contents of <0.4–4% in the pyroxene.

Plagioclase—Although our bulk sample shows higher Na and Al abundances than other samples, INAA on isolated plagioclase grains was not possible because plagioclase is generally small (5–10 μm).

However, plagioclase has to be considered to model the REE budget in bulk aubrites. Plagioclase is an important Eu carrier as seen from Fig. 8, which shows the available literature data for Eu and Na in bulk aubrite samples. The Eu abundances increase with increasing Na (albite) content. This trend is less developed for other REE. In samples with low Na contents Eu abundances are often higher than expected from the general correlation. All Peña Blanca Spring samples display higher Eu contents. Another Eu bearing phase, presumably oldhamite, dominates the bulk abundances. However, from the Na/Eu correlation we estimate an upper limit of about 0.5 ppm Eu (10x chondritic) for plagioclase, which is in the reported range of 5–14x chondritic from plagioclase ion probe analyses (Floss *et al.*, 1990; Wheelock, 1990).

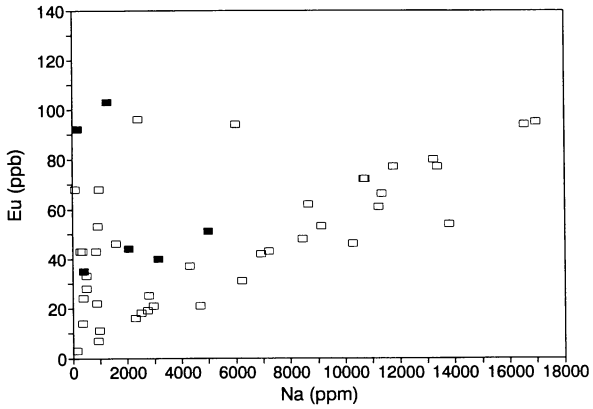

FIG. 8. Whole rock Eu and Na abundances in Peña Blanca Spring (filled symbols, data see Table 2 and 4) and other aubrites (Strait 1983). For samples with more than 2000 ppm Na, the Eu/Na correlation indicates that the majority of Eu is sited together with Na in plagioclase. This correlation allows us to estimate the Eu abundance in plagioclase to 0.5 ppm. For samples with low Na abundances a wide scatter of Eu abundances is found. Another Eu carrier, presumably oldhamite, dominates the bulk Eu abundances in samples with low plagioclase contents.

It is also interesting to note that the Sm/Eu fractionation is higher than that expected from equilibrium partitioning between plagioclase and melt. However, all available experimental plagioclase/liquid partition coefficients are determined for anorthite-rich plagioclase, and it is not known if larger Sm/Eu fractionations can be obtained for albite than for anorthite under the same fO_2 conditions.

IMPLICATIONS FOR THE AUBRITE PARENT BODY

The trace element systematics discussed in previous sections clearly indicate that nebular processes alone are not sufficient to explain bulk aubrite trace element patterns. Low contents of siderophile elements may be explained by incomplete accretion of metal to the parent body. However, an explanation of the depletions of the refractory elements (V, Cr, Ti) requires more sophisticated modeling, *i.e.*, sulfide removal during melting of the APB. Depending on the extent of heating of the APB, two extreme cases for melting can be envisioned: (1) high degrees of partial melting of the parent body leading to removal of metal and sulfides and formation of aubrites as residues from fractional crystallization (*e.g.*, Watters and Prinz, 1979; Okada *et al.*, 1988) or (2) a short melting episode where metal and sulfides were removed (non-equilibrium melting). Impacts may have provided the energy for the short melting episode.

In the first model, complete melting of the parent body is required and any primary signatures reflecting nebular condensation processes would be erased. In the second scenario, such inhomogeneities may survive a short melting episode and some relicts of primary solar nebula related processes may still be present in aubrites. As will be discussed below, the second model is more plausible because (1) the REE abundances in oldhamite strongly suggest that oldhamite gained its REE inventory during condensation in the solar nebula and

was only partially altered by processes on the APB, and (2) because the bulk aubrite REE budget cannot be explained by fractional crystallization processes.

Distribution and Significance of REE in Aubrites and the Origin of Oldhamite

The quantitative modeling of the REE abundances in a bulk aubrite sample requires the knowledge of the REE content in all phases and the modal abundances of these host phases. The present study, in combination with literature data, allows us to make quantitative calculations for the expected REE budget for the bulk sample analyzed. The REE bearing phases considered are oldhamite, plagioclase, enstatite, and diopside. The bulk REE abundances are calculated from the mass-balance equation:

$$C_{tot} = C_{old} F_{old} + C_{plag} F_{plag} + C_{dio} F_{dio} + C_{en} F_{en}$$

where C stands for concentration in the respective phases and F for weight fractions of minerals present in the bulk sample.

The fractions of mineral phases were derived as follows. The leaching experiments yield a CaS fraction of $F_{old} = 0.0027$ for the bulk sample. The undissolved Ca must be sited in diopside, because plagioclase is mainly albitic. The fraction of diopside is then calculated from EMP Ca data for diopside (Watters and Prinz 1979, Table 3) as $F_{dio} = 0.035$. The fraction of enstatite is derived similarly from the bulk Mg content minus the amount of Mg present in diopside as $F_{en} = 0.86$. The Al and Na abundances of the bulk sample combined with the analytical data on plagioclase from Watters and Prinz (1979) yield $F_{plag} = 0.07$. The REE abundances in plagioclase, diopside, and enstatite were taken from analyses of other aubrites (Wheelock, 1990; Floss 1991). For diopside, Floss (1991) reports two different REE abundance patterns. We used the data for diopside displaying a negative Eu-anomaly and an otherwise LREE to HREE enriched pattern in our calculations, however, no significant changes were obtained by using the data of the other diopside with a rather flat REE pattern and no Eu-anomaly. For oldhamite, we used the abundances from both oldhamite grains determined here. The results of the calculations are shown in Fig. 9. If only the REE in silicates are considered with no oldhamite present, the calculated pattern is heavy REE enriched (about 0.02 to 0.3x EH-chondrites) with a positive Eu anomaly (about 0.55x EH-chondritic). This pattern resembles the REE abundances found in the residue from the leaching experiment where about half of Eu remains in the residue (silicates) and light REE are higher in the leach than heavy REE (Fig. 5).

The addition of 0.27% (by mass) oldhamite with abundances as determined in the 0.097 mg grain produces a more or less flat REE abundance pattern with a small positive Eu anomaly. Except for Eu, the REE abundances are below the observed values. If oldhamite with REE abundances as in the 4.11 mg grain is added to the silicates, a bulk pattern with a negative Eu-anomaly is obtained. In this case, REE abundances (except for Eu) are slightly above the measured values. For Eu a good agreement between measured and calculated abundances is obtained in both cases. However, the predicted overall patterns either display a negative or positive Eu-anomaly, depending on the REE abundances in the oldhamite used for the mass balance calculations. For better estimates some understanding of the variations of REE in oldhamite is required.

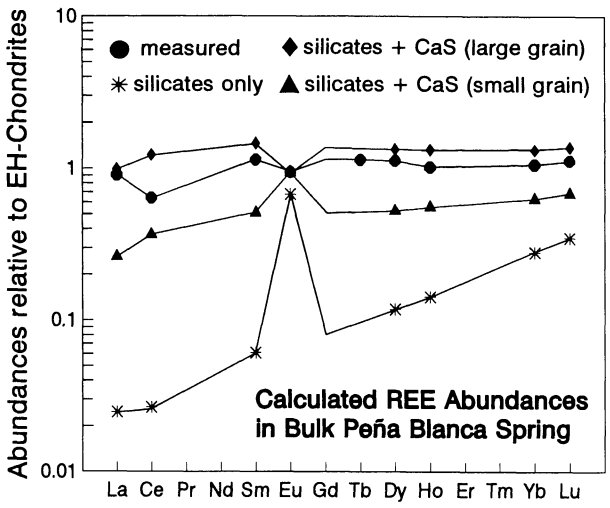

FIG. 9. Calculated REE abundances in bulk Peña Blanca Spring, see text for details. If only the REE in bulk silicates are considered, the bulk pattern displays LREE to HREE enrichment and a positive Eu-anomaly. This is consistent with the results from the leaching experiment (Fig. 5). Addition of 0.27% of oldhamite with REE abundances determined for the small or large grain increase bulk REE closer to observed values. However, except for Eu, in neither case a perfect match of calculated and measured REE pattern is obtained.

In earlier work we concluded that oldhamite in aubrites is not of igneous origin but is instead a metamorphosed relict condensate (Lodders and Palme, 1990). The REE abundance patterns in diopside and plagioclase were probably established during metamorphic events because these patterns are inconsistent with fractional crystallization. The major reasons for our conclusions that oldhamite is of non-igneous origin will be discussed in some detail in the following paragraphs.

Oldhamite is the main REE carrier in E-chondrites (*e.g.*, Larimer and Ganapathy, 1987; Lundberg and Crozaz, 1988; Chen *et al.*, 1989) and in aubrites (*e.g.*, Wolf *et al.*, 1983; Strait 1983, Benjamin *et al.*, 1984; Floss *et al.*, 1990, Wheelock *et al.*, 1990). In most cases, oldhamite in EH-, EL-chondrites and aubrites is highly enriched in REE by roughly a factor of about 100x chondritic. These enrichments are consistent with those predicted for REE condensation into CaS at the high C/O ratios required to form enstatite chondrites (*e.g.*, Larimer and Bartholomay, 1979; Lodders and Fegley, 1993). Oldhamite is calculated to be the first REE-bearing condensate and the REE completely condense into oldhamite before other potential REE host phases form. If all Ca condenses as CaS and the REE were completely incorporated in oldhamite, abundances of the REE of at least 60x chondritic are expected. A higher calculated level of REE and fractionations among the REE (such as Eu and Yb depletions or enrichments) are expected, depending on the temperature of oldhamite removal from the nebula gas (see Lodders and Fegley (1993) for details). Oldhamites displaying such REE anomalies have been reported by Floss (1991) for aubrites, a clear indication of a origin by condensation.

The large REE enrichments in aubritic oldhamite are not expected from igneous partitioning. Experimentally determined CaS/silicate partition coefficients for the REE (Dickinson *et al.*, 1990; Lodders *et al.*, 1990) are about 0.5 to 10 while partition coefficients of about 200 are required to explain the large REE

enrichments observed in oldhamite. Even if oldhamite/melt partition coefficients for the REE were much higher, and crystallization of CaS from a Mg-rich melt were possible, nearly complete extraction of all REE into a phase with a modal abundance of <0.5 wt% seems to be very unlikely, because it requires a perfectly efficient process. Crystallization of oldhamite from a late REE-enriched liquid could produce high REE concentrations in oldhamite despite low partition coefficients. However, this is unlikely because CaS is a very refractory mineral as shown below.

Aubrites probably formed from material similar to enstatite chondrites. Therefore oldhamite must have been present when the APB differentiated. Although temperatures on the APB are assumed to have been sufficiently high to melt enstatite (mp 1851 K), it is extremely unlikely that temperatures ever exceeded the pure CaS melting point (2723 ± 50 K, Medvedev *et al.*, 1979). It is also unlikely that temperatures approached the melting points of the oldhamite solid solutions observed in aubrites. Although no high temperature phase diagrams are available for these compositions, thermodynamic calculations of liquidus temperatures can be made assuming ideal solid solution using the relationship for melting point depression (*e.g.*, Denbigh, 1981):

$$T_m = T^*_m - (RT^{*2}_m/\Delta H_{fus})X_{FeS, MnS, MgS}$$

where T^*_m is the melting point of pure CaS, ΔH_{fus} is the heat of fusion (66940 ± 20900 J/mol; Medvedev *et al.*, 1979), and $X_{FeS, MnS, MgS}$ is the sum of mole fractions of FeS, MnS, and MgS derived from INAA data on oldhamite. A simple calculation shows that solid solutions of CaS with FeS, MnS, and MgS have high melting points (T_m) close to that of pure CaS. If we insert data we obtain a melting point of $T_m = 2620\ ^{+72}_{-92}$ K (the range results from uncertainties in the CaS melting point and in H_{fus}). This value is only about 100° below the melting point of pure CaS and reflects the very refractory nature of oldhamite in enstatite meteorites. Thus, CaS cannot be a late crystallizing phase.

Although oldhamite-plagioclase assemblages are observed in aubrites, CaS formation by sulfurization of plagioclase is implausible. One consequence of sulfurization is that FeO in silicates would be completely converted to FeS under the sulfur fugacities required for CaS formation. However, some FeO is still present in the silicates. Another consequence of sulfurization is that plagioclase grains with anorthite-rich centers and albite-rich rims should be produced. However, Wheelock (1990) measured albite and anorthite profiles of plagioclase coexisting with oldhamite and found exactly the opposite trend. Instead of plagioclase reacting to form oldhamite, it seems that oldhamite partially reacted with plagioclase forming anorthite enriched rims and leaving an albite rich center. We also note that the analytical data are inconsistent with fractional crystallization because anorthite crystallizes first and albite later.

Under the (T, fO_2) conditions of the APB, breakdown of oldhamite is more likely than its formation. Oldhamite, inherited from an E-chondrite-like parent body, will eventually form diopside (Fogel *et al.*, 1988). Reactions exemplified by $3MgSiO_3 + CaS + 1/2O_2 = CaMgSi_2O_6 + Mg_2SiO_4 + 1/2S_2$ may explain why diopside and forsterite occur in aubrites but not in E-chondrites. Indeed, more forsterite is observed in silicates of sulfide dominated clasts (Wheelock, 1990). Keil (1989) presented several arguments against this reaction. One argument is that the amount of oldhamite in enstatite chondrites (about 0.5%) is not sufficient to explain the diopside abundances of up to 20% in aubrites (Okada *et al.*, 1988). If all diopside formed from oldhamite, the maximum possible amount of diopside in aubrites is about 2.3%. This is close to or lower than the diopside abundances reported by Watters and Prinz (1979) for several aubrites. The large abundance of diopside described by Okada *et al.* (1988) for Norton County is rather exceptional (as is the 2-cm sized oldhamite grain found by Wheelock *et al.* (1990)) and may not be representative for the aubrites as a group. Keil's second argument is that the breakdown of oldhamite requires higher oxygen fugacities than those which may occur on a very reduced parent body. However, oxygen can be supplied by the conversion of the FeO or MnO in pyroxene to FeS and MnS. Indeed, pyroxene in enstatite chondrites contains more FeO and MnO than does pyroxene in aubrites (Keil, 1968; Watters and Prinz, 1979).

Diopside would also inherit the REE from oldhamite. Two different types of diopside REE patterns in Bustee and Bishopville have been reported (see above; Floss, 1991). In Norton County a LREE to HREE enriched pattern (1 to 10x chondritic) displaying a negative Eu-anomaly was found by Wheelock (1990). The shapes of these patterns are similar to those found in oldhamite in the respective meteorites. We suggest that these different patterns are due to the conversion of oldhamite to diopside. Oldhamite REE abundances of about 100x chondritic correspond to abundances of about 30x chondritic in diopside, if the conversion is complete. The two different REE patterns in diopside which resemble oldhamite REE patterns, and have REE abundances relatively close to the expected values support the suggestion that diopside formed by reaction of oldhamite. Diopside formation by fractional crystallization processes cannot explain the observed REE abundances nor the different REE patterns.

The REE and especially Eu, may be partly redistributed from oldhamite into plagioclase and troilite during metamorphic events. As discussed by Larimer and Ganapathy (1987) this redistribution will produce lower REE contents in oldhamite of meteorites with increasing metamorphic type. Smaller oldhamite grains are expected to be more affected by metamorphism because of their larger surface to volume ratio. Indeed, the smaller oldhamite grain analyzed here has a REE inventory three times lower than the larger grain. A redistribution of Eu must have occurred because incomplete condensation of the REE in the solar nebula would produce both Eu *and* Yb depletions in oldhamite (Lodders and Fegley, 1993). Although Eu is depleted in Peña Blanca Spring oldhamite, the more volatile Yb is enriched as the other HREE (Fig. 6). The preferential Eu redistribution from oldhamite to plagioclase may be tested by measuring zoning profiles of Eu in plagioclase from different lithologies. Profiles showing Eu enrichments at the rims should be present, like the anorthite rims which have been observed (Wheelock 1990).

Evidence for increasing degrees of metamorphism in the sequence EH-, EL-chondrites, and aubrites is also reflected by the Mn and Mg abundances in oldhamite (Larimer and Ganapathy, 1987). The Mn abundances in oldhamite increase from EH-chondrites through EL-chondrites to aubrites whereas Mg contents decrease (Keil, 1968; Watters and Prinz, 1979). This trend probably indicates various stages of incomplete equilibrium between oldhamite and other phases. In fact, we find a higher Mn content in the small grain compared to the

large grain, while Mg is below the detection limit (Table 5). The occurrence of alabandite and troilite as blebs in oldhamite from Norton County or Peña Blanca Spring does not necessarily imply that these phases were enclosed during igneous formation of oldhamite, as suggested by Wheelock *et al.* (1990), but may instead be due to low temperature immiscibility of these sulfides (Skinner and Luce, 1971).

One of the most frequently used arguments against the relict oldhamite hypothesis is the much larger grain size of oldhamite in aubrites than in E-chondrites (Wheelock *et al.*, 1990). However, very large oldhamite grains in aubrites, such as the 2-cm grain studied by Wheelock *et al.* (1990), are rare. Most oldhamite grains in Peña Blanca Spring are generally <1 mm in size. Assuming that the initial oldhamite in the APB parent body had similar grain sizes as oldhamite in E-chondrites (30–200 μm, Larimer and Ganapathy, 1987), sintering of CaS might have led to the formation of larger aggregates. In this regard we note the highly favorable surface energy minimization resulting from sintering of small grains and the short sintering times for small grains (Kingery *et al.*, 1976). The presence of a melt would provide a highly effective medium for mass transport during sintering analogous to the liquid sintering aids used in industrial ceramics processes. Because oldhamite is less dense than other sulfides or metal and silicate melts, it can be envisioned that some oldhamite grains float, accumulate and sinter together. During an experimental study of REE partitioning between CaS and silicate melt, CaS grains from the starting material sintered together to form large aggregates (Lodders *et al.*, 1990). Sintering should favor exchange reactions and indeed the smaller Peña Blanca Spring oldhamite grain does show lower REE abundances than the larger grain analyzed. However, the abundances observed are still much too high to reflect any significant crystal/melt equilibrium.

Indicators for Sulfide Separation on the APB

The amount of sulfide segregation on the APB can be estimated from the refractory chalcophile elements, Ti and V. Both elements are enriched in troilite (Table 3). Because only an upper limit for Ti could be determined in our bulk sample, Ti is not used in further calculations. Metal separation may also have affected the bulk V, Cr, and Mn abundances in Peña Blanca Spring as these elements become siderophile under very reducing conditions as well (Rammensee *et al.*, 1983; Drake *et al.*, 1989). Figure 10 gives the abundances of these elements in the bulk sample, in the troilite fractions, and the experimentally determined sulfide/silicate and metal/silicate partition coefficients under reducing conditions (Drake *et al.*, 1989). Sulfide/silicate partition coefficients are about a factor of 10 higher than metal/silicate partition coefficients. The pattern found for troilite more closely resembles the pattern expected from sulfide/silicate partitioning than from metal/silicate partitioning.

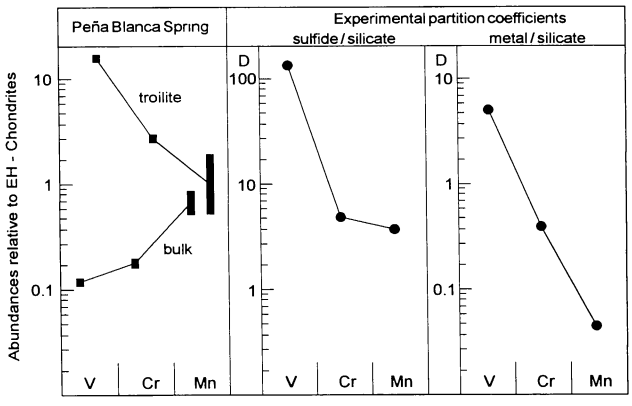

FIG. 10. V, Cr, and Mn abundances (relative to EH-chondrites) in bulk Peña Blanca Spring, in separated troilite grains, and sulfide/silicate and metal/silicate partition coefficients under reducing conditions (1260 °C, log fO_2 = −16.4, Drake *et al.*, 1989). The higher sulfide/silicate partition coefficients and their resembling pattern to troilite V, Cr, and Mn relative abundances suggest enrichment of these elements in sulfide rather than metal.

We can use the V abundances in bulk Peña Blanca Spring and in mineral separates to calculate the fraction of sulfide removed F_{sulf} as:

$$F_{sulf} = (C_{tot} - C_{sil})/(C_{sulf} - C_{sil}).$$

We assume an enstatite chondritic V abundance for the APB (C_{tot} = 55 ppm). The concentration for the APB silicate portion is given by the V abundance found in aubrites (C_{sil} = 6.5 ppm). Because the aubritic V abundance is mainly determined by small troilite grains enclosed in the whole rock sample, this calculation will only give a lower limit for the amount of sulfide separated. We take the V abundance in the troilite (c_{sulf} = 795 ppm) as representative of the V abundance in sulfides which separated on the APB. From the equation above we calculate that about 6% (by mass) sulfide must have been removed. A similar calculation could be made for Cr. However, Cr is present in troilite, alabandite, daubreelite, and other sulfide phases and for the mass balance calculation some knowledge of the Cr abundance in the "bulk sulfide" is also required.

Indicators for Metal Separation on the APB and the Source Material for Aubrites

Metal separation on the APB is reflected by the low abundances of highly siderophile elements such as Au and Ir in aubrites. Both elements are highly depleted in bulk samples and the concentrations found are primarily due to the presence of tiny metal grains left behind from metal segregation. In a recent study on aubritic metal compositions Casanova *et al.* (1993) also postulated the need for a metal core formation event in the APB. These authors concluded that the minimum metal content of the APB is not unlike that of enstatite chondrites.

Casanova *et al.* (1993) used partition coefficients to calculate the metal fraction of the APB. A different approach to determine the amount of metal which segregated on the APB is to perform a mass balance calculation similar to that done for sulfide fractionation above. We assume that the whole APB has EH or EL-chondritic Ir (and Au) abundances. We use average Ir and Au abundances in metal from aubrites (Casanova *et al.*, 1993), because no Ir and Au analyses of metal from Peña Blanca Spring are available. We obtain a lower limit of 23–25% (by mass) metal segregation on the APB, which is in the range of 20–30% metal segregation determined by Casanova *et al.* (1993). An abundance of 25% metal in the APB would imply that the APB is closer to EH-chondritic composition than EL-chondritic composition (average 18.9% and EH 23.5%; Keil, 1968).

Other mineral occurrences and compositions also indicate that the APB was closer in composition to EH-chondrites than to EL-chondrites. Plagioclase composition in aubrites (Ab_{93}) and EH-chondrites (Ab_{95}) are very similar but distinct from EL-chondritic (Ab_{81}; data from Watters and Prinz, 1979; Keil 1968). The occurrence of djerfisherite and caswellsilverite in both, EH-chondrites and aubrites, but not in EL-chondrites also suggests closer compositional similarities of the aubrite and EH-chondrite parent bodies. On the other hand, the occurrence of niningerite, (Mg,Fe)S, in EH-chondrites only and the restricted occurrence of alabandite in EL-chondrites and aubrites do not argue against an EH-relationship of aubrites as niningerite is not stable at the higher metamorphic temperatures of the EL-chondrite and aubrite parent bodies while alabandite is probably a product of metamorphism (Keil, 1968, 1989).

CONCLUSIONS

Results of analyses presented in this work in combination with literature data provide a more detailed picture of the evolution of the APB than was previously available. The low abundances of chalcophile (V, Ti) and siderophile elements (Au, Ir) in bulk aubrites and the REE distribution in aubritic minerals suggest that the APB underwent a short melting episode which was sufficient to form a core by metal and sulfide segregation but not sufficient to allow complete phase equilibria. The amount of sulfide (6%) and metal (25%) separated are in the range of metal and sulfide contents of EH-chondrites, indicating that the APB is closer to EH-chondritic composition. The INAA data on bulk samples, mineral separates and the results of a leaching experiment allow us to perform mass balance calculations for the REE. The main REE carrier is oldhamite, which originally contained the REE from condensation. The Mn and Mg abundances in oldhamite and the high but variable level of REE abundances indicate that exchange reactions of oldhamite with other phases have occurred. The REE were partially redistributed to other phases with Eu being preferentially removed into plagioclase. Some of the initially present, presumably small oldhamite grains were converted to diopside. The REE distribution among the silicates is inconsistent with fractional crystallization.

Acknowledgments—We thank B. Spettel for data on one bulk analysis of Peña Blanca Spring and his help with INAA procedures, and G. Dreibus for S-analysis on the whole rock sample. We also thank Th. Ntaflos for comments and B. Fegley for several helpful discussions. During final work on this paper, K. L. was supported by grants from the NASA Origins of the Solar Systems and Planetary Atmospheres Programs (B. Fegley P. I.). Samples were irradiated at the TRIGA Mark II reactor of the Institut für anorganische Chemie and Kernchemie der Johannes-Gutenberg Universität, Mainz, and we thank the reactor staff for technical support.

Editorial handling: R. Jones

REFERENCES

Benjamin T. M., Duffy C. J., Maggiore C. J., Rogers P. S. Z., Woolum D. S., Burnett D. S. and Murrell M. T. (1984) Microprobe analysis of rare earth element fractionation in meteoritic minerals. *Nucl. Inst. Meth. Phys. Res.* **B3**, 677–680.

Biswas S., Walsh T., Bart G. and Lipschutz M. E. (1980) Thermal metamorphism of primitive meteorites–XI. The enstatite meteorites: Origin and evolution of a parent body. *Geochim. Cosmochim. Acta* **44**, 2097–2110.

Casanova I., Keil K. and Newsom H. E. (1993) Composition of metal in aubrites: Constraints on core formation. *Geochim. Cosmochim. Acta* 57, 675–682.

Chen Y., Pernicka E., Lin Y. and Wang D. (1989) REE and some other trace element distribution of oldhamite in Qingzhen (EH3) chondrite (abstract). *Meteoritics* **24**, 259.

Denbigh K. (1981) *The Principles of Chemical Equilibrium.* Cambridge Univ. Press, Cambridge. U. K. 494 pp.

Dickinson T. L., Lofgren G. E. and McKay G. A. (1990) REE partitioning between silicate liquid and immiscible sulfide liquid: The origin of the negative Eu anomaly in aubrite sulfides (abstract). *Lunar Planet. Sci.* **21**, 284–285.

Drake M. J., Newsom H. E. and Capobianco C. J. (1989) V, Cr, and Mn in the Earth, Moon, EPB, and SPB and the origin of the Moon: Experimental studies. *Geochim. Cosmochim. Acta* **53**, 2101–2111.

Easton A. J. (1985) Seven new bulk chemical analyses of aubrites. *Meteoritics* **20**, 571–573.

Easton A. J. (1986) Studies of kamacite, perryite and schreibersite in E-chondrites and aubrites. *Meteoritics* **21**, 79–93.

El Goresy A., Grögler N. and Ottemann J. (1974) Djerfisherite composition in Bishopville, Peña Blanca Springs, St. Marks and Toluca meteorites. *Chem. Erde* **30**, 77–82.

Floss C. (1991) Rare earth element and other trace element microdistributions in two unusual extraterrestrial igneous systems: The enstatite achondrite (aubrite) meteorites and the lunar ferroan anorthosites. Ph. D. thesis, Washington Univ., 253 pp.

Floss C., Strait M. M. and Crozaz G. (1990) Rare earth elements and the petrogenesis of aubrites. *Geochim. Cosmochim. Acta* **54**, 3553–3558.

Fogel R. A. (1988) The enstatite chondrite-aubrite link (abstract). *Lunar Planet. Sci.* **19**, 343–344.

Fuchs L. H. (1974) Glass inclusions of granitic compositions in orthopyroxenes from three enstatite achondrites (abstract). *Meteoritics* **9**, 342.

Gibson E. K., Moore C. B., Primus T. M. and Lewis C. F. (1985) Sulfur in achondritic meteorites. *Meteoritics* **20**, 503–511.

Jarosewich E., Nelen J. A. and Norberg J. A. (1980) Reference samples for electron microprobe analysis. *Geostandards Newsletter* **4**, 43–47.

Kallemeyn G. W. and Wasson J. T. (1986) Compositions of enstatite (EH3, EH4,5 and EL6) chondrites: Implications regarding their formation. *Geochim. Cosmochim. Acta* **50**, 2153–2164.

Keil K. (1968) Mineralogical and chemical relationships among enstatite chondrites. *J. Geophys. Res.* **73**, 6945–6976.

Keil K. (1989) Enstatite meteorites and their parent bodies. *Meteoritics* **24**, 195–208.

Kingery W. D., Bowen H. K. and Uhlman D. R. (1976) *Introduction to Ceramics*. J. Wiley, New York. pp. 1032.

Kruse H. (1979) Spectra processing with computer graphics. *Mayaguez Conf. Proc.*, United States Dept. of Energy (DOE) Report 78421, 76–84.

Larimer J. W. and Bartholomay M. (1979) The role of carbon and oxygen in cosmic gases: Some applications to the chemistry and mineralogy of enstatite chondrites. *Geochim. Cosmochim. Acta* **32**, 965–982.

Larimer J. W. and Ganapathy R. (1987) The trace element chemistry of CaS in enstatite chondrites and some implications regarding its origin. *Earth Planet. Sci. Lett.* **15**, 123–134.

Larimer J. W. and Wasson J. T. (1988) Refractory lithophile elements. In *Meteorites and the early solar system* (eds. J. F. Kerridge and M. S. Matthews), pp. 394-415. Univ. Arizona Press, Tucson, Arizona.

Lodders K. and Fegley B. (1993) Lanthanide and actinide chemistry at high C/O ratios in the solar nebula. *Earth Planet. Sci. Lett.* **117**, 125–145.

Lodders K. and Palme H. (1990) Fractionation of REE during aubrite formation: The influence of FeS and CaS (abstract). *Lunar Planet. Sci.* **21**, 710–711.

Lodders K. and Palme H. (1991) The role of sulfur in planetary core formation (abstract). *Meteoritics* **26**, 366.

Lodders K., Palme H. and Drake M. J. (1990) The origin of oldhamite in enstatite achondrites (aubrites). (abstract). *EOS* **71**, 1434.

LONSDALE J. T. (1947) The Peña Blanca Spring meteorite, Brewster County, Texas. *Am. Mineral.* **32**, 354–364.

LUNDBERG L. L. AND CROZAZ G. (1988) Enstatite chondrites: A preliminary ion microprobe study (abstract). *Meteoritics* **23**, 285–286.

MEDVEDEV V. A., BERGMAN G. A., GURVICH L. V., YUNGMAN V. S., VOROBIEV A. F. AND KOLESOV V. P. (1979) *Termicheskie Konstanty, Veshchastv (Thermal Constants of Substances), Be, Mg, Ca, Sr, Ba, Ra* (ed. V. P. Glusko) Part IX, Akad. Nauk USSR, Viniti, Moscow. 522 pp.

OKADA A., KEIL K. AND TAYLOR G. J. (1981) Unusual weathering products of oldhamite parentage in the Norton County enstatite achondrite. *Meteoritics* **16**, 141–152.

OKADA A., KEIL K., Taylor G. T. AND NEWSOM H. (1988) Igneous history of the aubrite parent asteroid: Evidence from the Norton County enstatite achondrite. *Meteoritics* **23**, 59–74.

PALME H., LARIMER J. W. AND LIPSCHUTZ M. E. (1988) Moderately volatile elements. In *Meteorites and the early solar system* (eds. J. F. Kerridge and M. S. Matthews), pp. 436-461. Univ. Arizona Press, Tucson, Arizona.

RAMMENSEE W., PALME H. AND WÄNKE H. (1983) Experimental investigation of metal-silicate partitioning of some lithophile elements (abstract). *Lunar Planet. Sci.* **14**, 628–629.

REID A. M. AND COHEN A. J. (1967) Some characteristics of enstatite from enstatite achondrites. *Geochim. Cosmochim. Acta* **31**, 661–672.

SCHMITT R. A., SMITH R. H. AND OLEHY D. A. (1972) Element abundances in stony meteorites. *Meteoritics* **7**, 131–213.

SEARS D. W., KALLEMEYN G. W. AND WASSON J. T. (1983) Composition and origin of clasts and inclusions in the Abee enstatite chondrite. *Earth Planet. Sci. Lett.* **62**, 180–192.

SHIMA M. AND HONDA M. (1967) Distribution of alkali, alkaline earth, and rare earth elements in component minerals of chondrites. *Geochim. Cosmochim. Acta* **31**, 1995–2006.

SKINNER B. J. AND Luce F. D. (1971) Solid solutions of the type (Ca, Mg, Mn, Fe)S and their use as geothermometer for the enstatite chondrites. *Amer. Mineral.* **56**, 1269–1296.

STRAIT M. M. (1983) Chemical variations in enstatite achondrites. Ph. D. thesis, Arizona State Univ., 172 pp.

WÄNKE H., KRUSE H., PALME H. AND SPETTEL B. (1977) Instrumental neutron activation analysis of lunar samples and the identification of primary matter in the lunar highlands. *J. Radioanal. Chem.* **38**, 363–378.

WASSON J. T. AND KALLEMEYN G. W. (1988) Composition of chondrites. *Phil. Trans. R. Soc. Lond.* **A325**, 535–544.

WASSON J. T. AND WAI C. M. (1970) Composition of the metal, schreibersite and perryite of enstatite achondrites and the origin of enstatite chondrites and achondrites. *Geochim. Cosmochim. Acta* **34**, 169–184.

WATTERS T. R. AND PRINZ M. (1979) Aubrites: Their origin and relationship to enstatite chondrites. *Proc. Lunar Planet. Sci. Conf.* **10th**, 1073–1093.

WHEELOCK M. M. (1990) The magmatic history of an aubrite parent asteroid: Evidence from igneous clasts and trace elements. MS Thesis, Univ. of New Mexico, 78 pp.

WHEELOCK M. M., HEAVILON C. F. AND KEIL K. (1990) An ion probe study of REE distribution in sulfide and silicate minerals in the Norton County aubrite (abstract). *Lunar Planet. Sci.* **21**, 1327–1328.

WILSON L. AND KEIL K. (1991) Consequences of explosive eruptions on small solar system bodies: The case of the missing basalts on the aubrite parent body. *Earth Planet. Sci. Lett.* **104**, 505–512.

WOLF R., EBIHARA M., RICHTER G. R. AND ANDERS E. (1983) Aubrites and diogenites: Trace element clues to their origin. *Geochim. Cosmochim. Acta* **47**, 2257–2270.